Transition Metal Chemistry (2005) 30:404–410
DOI 10.1007/s11243-004-6972-5

Biomimetic oxovanadium(IV) and (V) complexes with a tridentate (N,N,O)-donor hydrazonic ligand. Two X-ray crystal structure modifications of (2-acetylpyridine-benzoylhydrazonato)dioxovanadium(V)

Pedro Ivo da S. Maia, Victor M. Deflon*, Elizeu J. de Souza, Edgardo Garcia and Gerimário F. de Sousa
Instituto de Química, Universidade de Brasília, BR - 70919-970 Brasília - DF, Brazil

Alzir A. Batista and Alberthmeiry T. de Figueiredo
Departamento de Química, Universidade Federal de São Carlos, BR - 13565-905 São Carlos - SP, Brazil

Elke Niquet
Institut für Anorganische Chemie der Universität Tübingen, D - 72076 Tübingen, Germany

Received 30 September 2004; accepted 17 November 2004

Abstract

Two oxovanadium(IV) and (V) complexes with 2-acetylpyridine-benzoylhydrazone have been prepared and characterized. The analytical methods used included elemental analysis, i.r., FAB^+ m.s., ^{51}V-n.m.r. and e.p.r. X-ray diffractometry from single crystals as well as from microcrystalline material were also performed. Molecular modeling was used to calculate the complex structures in a vacuum and their vibrational frequencies. Octahedral coordination is suggested for the complex acetylacetonato(2-acetylpyridine-benzoylhydrazonato)-oxovanadium(IV) *(1)*, for which good agreement was verified between calculated and observed i.r. data. Two crystal structure modifications of (2-acetylpyridine-benzoylhydrazonato)dioxovanadium(V) *(2)* have been determined by X-ray diffraction methods. In both crystalline modifications the molecular structure of the complex shows a distorted trigonal bipyramidal VN_2O_3 coordination. The molecular structure, found experimentally for *(2)*, was compared with the theoretically calculated one. The results validate the theoretical method.

Introduction

Oxovanadium(IV) and (V) complexes, especially with bi- and tridentate chelating ligands bound to the metal mainly *via* oxygen and nitrogen atoms, have being extensively investigated in recent years with respect to their remarkable efficiency as insulin mimetic compounds [1–3]. Their use as orally active medicaments would represent an important advance in the treatment of human *diabetes mellitus*. Other studies involving potential applications of oxovanadium complexes have been also performed, with emphasis, for example, in their antitumor [4] and antibacterial [5] activity. The bioactivity of heterocyclic hydrazones as well as of their metal complexes is of interest, especially due to their pharmacological properties. In previous work we described oxo- and dioxovanadium complexes with the ligand 2-acetylpyridine-furanoylhydrazone (Hapf) [6]. A recent study showed that the analogous compound 2-acetylpyridine-benzoylhydrazone (Hapb) has antitubercular activity, which proved to be enhanced upon copper complexation [7].

The following coordination compounds with apb^{1-} as ligand, [VO(acac)(apb)] *(1)* and $[VO_2(apb)]$ *(2)*, are described in the literature, included between diverse biomimetic vanadium(IV) and (V) complexes [8]. New results involving the complexes *(1)* and *(2)* are presented here. The molecular structure of *(1)* was successfully calculated by molecular modeling. A comparison between observed and calculated i.r. bands is included. A new triclinic crystal structure modification of *(2)* was determined by X-ray structural analysis.

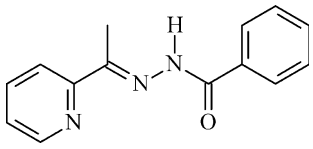

Hapb

Experimental

Materials

$[VO(acac)_2]$ (Aldrich) and analytical grade solvents were used as purchased. Hapb was prepared as previously described for Hapf [6].

* Author for correspondence

Instrumental

I.r. spectra were recorded on a BOMEM FT-IR model BM 100 spectrometer. ^{51}V-n.m.r. spectra in $CDCl_3$ were measured on a Varian Mercury Plus instrument, referring to $VOCl_3$ using aqueous NH_4VO_3 (−541.2 ppm for VO_4^{3-}) as an external secondary reference. Elemental analyses (CHN) were determined with FISONS EA-1108 equipment. E.p.r. spectra were collected on a VARIAN E109-110 spectrometer. Magnetic susceptibilities were measured on a JOHNSON MATTHEY MSB balance. A BAS 100B electrochemical analyzer was used for the cyclic voltammetry studies. Routine FAB^+ mass spectra have been recorded on a TSQ spectrometer (Finnigan) with *m*-nitrobenzyl alcohol as matrix. Enraf-Nonius CAD4 diffractometers with graphite monochromators were used for the X-ray structure analyses. Powder diffraction diagrams were obtained on a Rigako D/Max 2 A/C diffractometer (Cu/Kα; scan rate 1° min^{-1}) with a graphite monochromator.

Preparation of the vanadium complexes

Acetylacetonato(2-acetylpyridine-benzoylhydrazonato)-oxovanadium(IV) (1)

A solution of Hapb (0.120 g, 0.5 mmol) in MeOH (10 cm^3) was added to a solution of $[VO(acac)_2]$ (0.133 g, 0.5 mmol) in the same volume of MeOH. The mixture was stirred for 30 min. The green precipitate which formed was filtered off, washed with a little MeOH and dried under reduced pressure. Yield: 66%. M.p. was not observed below 300 °C. (Found: C, 55.6; H, 4.7; N, 10.3. $C_{19}H_{19}N_3O_4V$ calcd.: C, 56.4; H, 4.7; N, 10.4%).

(2-Acetylpyridine-benzoylhydrazonato)dioxovanadium-(V) (2)

An initially green solution of $[VO(acac)_2]$ (0.106 g, 0.4 mmol) and Hapb (0.096 g, 0.4 mmol) in MeOH (60 cm^3) was held at room temperature for 5 days with constant stirring, forming a yellow-brown solution with a yellow precipitate. The solvent was completely removed by heating and the crude product was submitted to re-crystallization in MeOH at −15 °C. After a few days, the mixture of yellow and red crystals was filtered off, washed with a little MeOH and dried under reduced pressure. Yield: 77%. M.p. was not observed below 300 °C. (Found: C, 51.9; H, 3.7; N, 12.9. $C_{14}H_{12}N_3O_3V$ calcd.: C, 52.3; H, 3.8; N, 13.1%).

X-ray crystal structure determinations

The X-ray structure determination from two different crystals, obtained from a solution of *(2)* in MeOH, revealed two different crystal structure modifications for the complex. A yellow triclinic structure modification was found in addition to the red monoclinic structure cited for the complex in the literature [8]. Crystal data and detailed information about the structure determinations are given in Table 1. Labeled diagrams of the monoclinic and triclinic structure modifications of *(2)* are shown in Figures 1 and 2, respectively. Selected bond lengths and angles are given in Table 2. The powder diffractogram of *(2)* was measured and compared with the X-ray powder patterns calculated from the single crystal data, obtained for both structure modifications, with the program POWDERCELL [9]. The data could be indexed in the monoclinic modification with the program DICVOL91 [10]. The cell constants calculated from the diffractogram data are given in Table 3, together with the indexed reflections. The microcrystalline material does not contain the triclinic modification, consisting in the monoclinic structure. The observed and calculated diagrams are given in Figure 3. The powder diagram was measured at 20 °C while the data collections for the single crystal structure determinations were performed at −65 °C and at −60 °C, for the monoclinic and triclinic modifications, respectively. Consequently, a shift between measured and calculated peaks is observed.

Theoretical calculations

Calculations were performed using a perturbative Becke-Perdew density functional model with a numerical polarization basis set [15] abbreviated as pBP/DN* as implemented in the software PC Spartan v1.0.5 [16]. Both structures had their geometry fully optimized and a frequency calculation was performed at the same level of theory.

Results and discussion

I.r. spectroscopy

The coordination of the hydrazone ligand monoanionically as apb^{1-} in *(1)* and *(2)* is indicated by the absence of absorption band characteristic for ν(N—H), found at 3179 cm^{-1} for Hapb, in their i.r. spectra. The *N,N,O*-coordination of the apb^{1-} ligand in *(1)* and *(2)* is evident. The bands found for ν(C=O) at 1655 cm^{-1}, ν(C=C + C=N) at 1580 and 1544 cm^{-1}, and ν(C—C + C—N) at 1466 and 1432 cm^{-1} in the free Hapb ligand are shifted in the spectra of both products. The coordinated $acac^{1-}$ ligand in *(1)* is confirmed by the presence of its characteristic ν(C—O) bands at 1522 and 1391 cm^{-1}. The strongest absorption band for each complex corresponds to ν(V=O), with values of 958 cm^{-1} for *(1)* and 944 cm^{-1} for *(2)*. More detailed information referring to the i.r. spectra of *(1)* and *(2)* are given in Table 4 and Table 6, respectively.

N.m.r. spectra

The ^{51}V-n.m.r. spectrum of *(2)* in $CDCl_3$ shows only a single peak at −476.7 ppm, consistent with the

Table 1. Crystal data and structure refinements for $[VO_2(apb)]$ *(2)*

Modification	Monoclinic	Triclinic
Empirical formula	$C_{14}H_{12}N_3O_3V$	$C_{14}H_{12}N_3O_3V$
Formula weight	321.21	321.21
Temperature (°C)	−65(2)	−60(2)
Wavelength (pm)/radiation	71.073 / MoK_α	154.184 / CuK_α
Space group	C2/c	$P\bar{1}$
Unit cell parameters		
a (pm)	1632.0(3)	768.40(5)
b (pm)	1270.46(11)	776.01(3)
c (pm)	1488.7(2)	2326.17(16)
α (°)	90	88.496(4)
β (°)	119.918(10)	88.526(6)
γ (°)	90	87.391(6)
V (pm^3)	$2675.4(7) \times 10^6$	$1384.73(14) \times 10^6$
Z	8	4
Absorption coefficient (mm^{-1})	0.755	6.123
Crystal size (mm)	$0.25 \times 0.15 \times 0.15$	$0.20 \times 0.10 \times 0.05$
Method / θ range (°)	ω scans / 3.03 to 27.97	ω scans / 5.71 to 65.01
Index ranges (h, k, l)	−1→21, −1→16, −19→17	−1→9, −8→9, −27→27
Collected reflections	3866	5711
Unique reflections / R_{int}	3220 / 0.0747	4644 / 0.0752
Observed data [$I > 2\sigma$ (I)]	1572	3627
Absorption correction	ψ-scans [11]	ψ-scans [11]
Min. / max. transmission	0.86715 / 0.91862	0.83739 / 0.98168
Structure refinement	Full-matrix least-squares on F^2	Full-matrix least-squares on F^2
Weighting scheme	$w = 1/[\sigma 2(F_o^2) + (0.0493P)^2]$ $P = (F_o^2 + 2F_c^2)/3$	$w = 1/[\sigma^2(F_o^2) + (0.0463P)^2 + 1.44P]$ $P = (F_o^2 + 2F_c^2)/3$
Hydrogen treatment	Fourier-map	Fourier-map
Refined parameters	238	476
Structure factors [$I > 2\sigma(I)$]	$R_1 = 0.0604$, $wR_2 = 0.1089$	$R_1 = 0.0441$, $wR_2 = 0.1050$
Goodness-of-fit, S	0.983	1.033
Extinction coefficient	not refined	0.00038(15)
Programs used	SIR92 [12] and SHELXL97 [14]	SHELXS97 [13] and SHELXL97 [14]

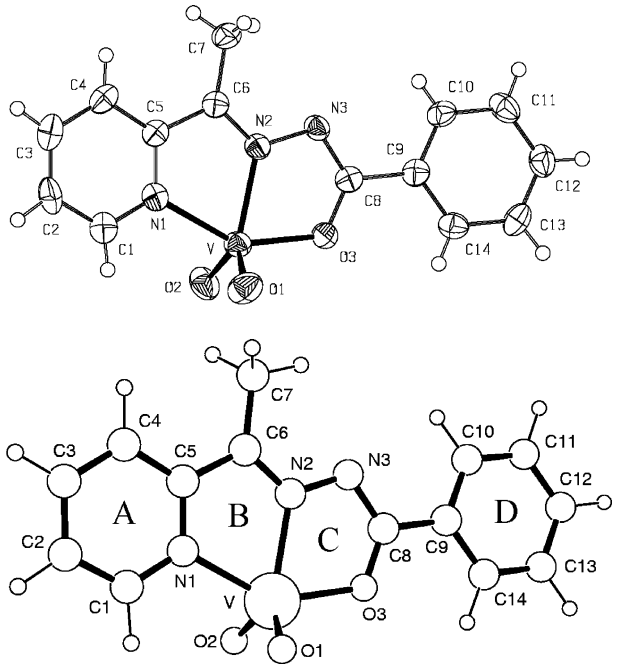

Fig. 1. ORTEP plot of $[VO_2(apb)]$ *(2)* in its monoclinic modification at the 50% probability level (top) and the theoretically calculated molecular structure (bottom).

pentacoordinate dioxovanadium(V) complex. There is no experimental evidence for the formation of an additional dinuclear complex, either in solution or in the solid state, as observed for the analog compound with the 2-acetylpyridine-furanoylhydrazonato(1−) anion [6] instead of the benzoyl derivative as the tridentate ligand.

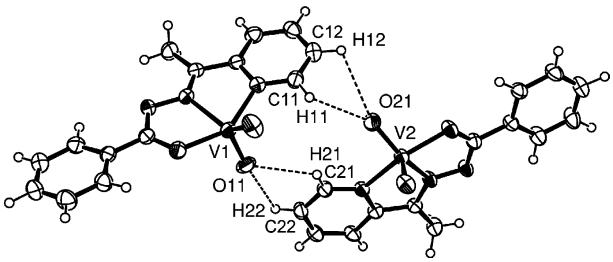

Fig. 2. ORTEP plot of two molecules of $[VO_2(apb)]$ *(2)* in its triclinic modification at the 50% probability level. The dashed bonds indicate die hydrogen bonds, with the following distances (pm) and angles (°): C(12)—O(21) = 3.239(5); H(12)—O(21) = 2.78(4); C(12)—H(12)···O(21) = 109(3); C(11)—O(21) = 3.062(5); H(11)—O(21) = 2.46(4); C(11)—H(11)···O(21) = 121(3); C(21)—O(11) = 3.232(4); H(21)—O(11) = 2.61(4); C(21)—H(21)···O(11) = 127(3); C(22)—O(11) = 3.328; H(22)—O(11) = 2.74(3); C(22)—H(22)···O(11) = 122(3).

Electrochemistry

The oxovanadium(IV) complex *(1)* oxidizes slowly in dilute alcoholic solution to the dioxovanadium(V) complex *(2)*, with loss of acetylacetone. The anodic peak related to the irreversible oxidation process of *(1)* is seen in its cyclic voltammogram at 821 mV (Figure 4).

Table 2. Selected bond lengths (pm) and angles (°) refined from X-ray data and calculated for [VO_2(apb)] *(2)*

Modification	Monoclinic	Triclinic*	Calcd. in a vacuum
Bond lengths			
V—O(1)	161.5(3)	161.8(3) / 162.1(3)	163.4
V—O(2)	161.4(3)	161.3(3) / 161.2(3)	163.3
V—O(3)	195.6(3)	194.8(2) / 194.8(2)	200.4
V—N(1)	211.5(3)	210.7(3) / 210.6(6)	214.6
V—N(2)	210.9(3)	210.1(3) / 209.9(3)	218.3
C(6)—N(2)	129.5(5)	129.0(5) / 129.7(4)	131.6
N(2)—N(3)	137.8(4)	138.3(4) / 137.6(4)	134.7
N(3)—C(8)	131.8(5)	130.8(5) / 131.9(4)	134.6
C(8)—O(3)	129.8(5)	130.3(4) / 131.3(4)	129.4
Bond angles			
O(1)—V—O(2)	110.44(18)	109.69(16) / 109.22(14)	110,96
O(1)—V—N(2)	123.86(16)	115.25(13) / 138.34(14)	124.97
O(2)—V—N(2)	125.21(16)	134.57(15) / 112.02(13)	122.91
N(1)—V—O(3)	146.30(14)	146.23(12) / 144.89(10)	144.88
N(1)—V—N(2)	72.87(14)	73.14(11) / 73.41(10)	72.45
O(3)—V—N(2)	73.43(12)	73.98(11) / 73.96(10)	72.46

* Values for two independent molecules in the asymmetric unit.

Table 3. Indexed reflections from the powder diagram data of [VO_2(apb)] *(2)*

hkl Indices	2θ	d	Intensity
110	8.786	10.06458	92
21−1	12.494	7.08469	58
020	13.102	6.75726	91
12−1	14.941	5.92943	25
211	18.173	4.88154	19
310	18.941	4.68531	66
22−2	19.500	4.55224	15
40−2	21.350	4.16178	39
320	22.136	4.01575	46
311	23.510	3.78408	100
013	24.280	3.66579	8
33−2	26.199	3.40147	38
51−2	27.037	3.29792	68
142	32.758	2.73385	11
104	34.638	2.58966	10

Magnetic measurements

The oxidation state +IV for the vanadium atom in *(1)* was experimentally confirmed. The compound is paramagnetic (d^1), with $\mu_{eff.} = 1.62\ \mu_B$ at 20 °C. It's anisotropic e.p.r spectrum in $CHCl_3$ solution is presented in Figure 5. Complex *(2)* is diamagnetic, with a silent e.p.r. signal.

Mass spectrometry

The FAB^+ m.s. spectrum of *(1)* in a *m*-nitrobenzyl alcohol matrix shows a *m*/*z* peak at 404.0, corresponding to $[VO(C_5H_7O_2)(C_{14}H_{12}N_3O)]^+$ (404).

Crystal structure modifications of (2-acetylpyridinebenzoylhydrazonato)dioxovanadium(V) (2)

Complex *(2)* presents a pentacoordinate vanadium(V) center. Both crystal structure modifications show the same molecular structure for the complex, with the oxo ligands in a *cis* conformation. The Hapb ligand coordinates N,N,O-tridentate and monoanionically as apb^{1-}. The C—C, C—O and C—N bond lengths show considerable double bond character and are consistent with an electron density delocalization among the nearly planar ligand. The phenyl ring is somewhat twisted in relation to the rest of the ligand. For the monoclinic structure the torsion angle is of 8.5(2)°. For the triclinic structure values of 8.4(1) and 6.9(1) are found for two independent molecules. The greatest deviations from the planarity of the apb^{1-} ligand, excluding the phenyl ring, are found for atom C(3) [4,6(4) pm] in the monoclinic

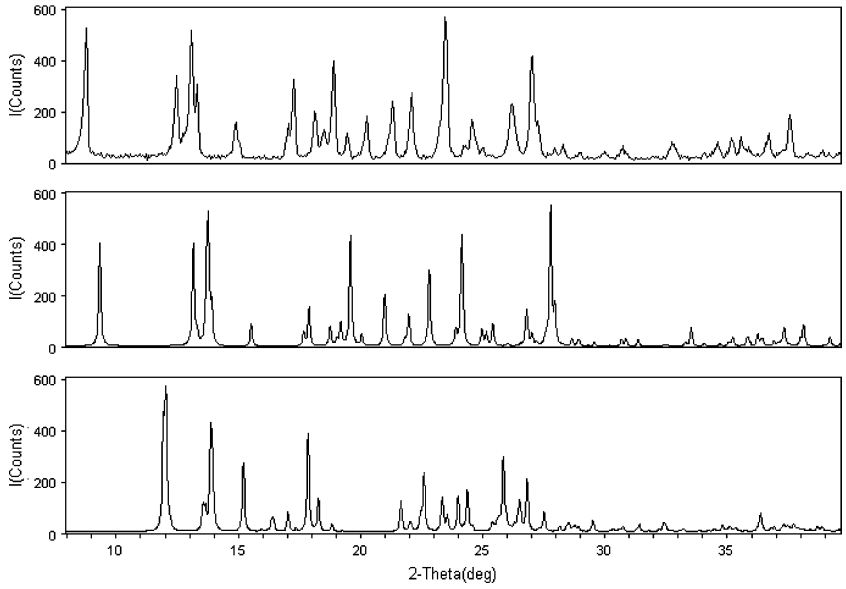

Fig. 3. Observed (top) and calculated powder diagrams for [VO(acac)(apb)] *(1)* in the monoclinic (middle) and triclinic (bottom) modifications.

Table 4. Observed and calculated i.r. absorptions bands in the fingerprint region (1600–400 mm^{-1}) for [VO(acac)(apb)] *(1)*, whose structure with labeled rings is shown in Figure 6

Assignment	Obs.	Calcd.
$\nu(C_6{=}N_2 + C_{10}{=}C_{11} + C_{13}{=}C_{14})$	1598 s	1591
$\nu(C_6{=}N_2) + \delta$(ring D)	1565 m	1568
$\nu(C_{18}{-}O_5 + C_{16}{-}O_4)$	1522 vs	1563
$\nu(C_8{-}C_9) + \delta$(C—H ring D)	1491 s	1465
$\nu(C_8{-}O_3 + C_8{-}N_3 + C_5{-}C_6)$ + δ(C—H rings A & D)	1463 s	1455
$\nu(C_8{-}O_3 + C_5{-}C_6) + \delta$(C—H rings A & D)	1426 vs	1437
$\nu(C_{18}{-}O_5 + C_{16}{-}O_4) + \delta(C_{15} + C_{19})$	1391 s	1398
$\nu(C_8{-}C_9 + C_6{-}C_7) + \delta$(C—H rings A & D)	1374 vs	1363
$\nu(C_5{-}C_6 + C_8{-}N_3)$	1321 m	1315
$\nu(C_5{-}N_1 + C_1{-}N_1)$	1302 ms	1306
δ(C—H rings A & D)	1270 m	1276
$\nu(C_{16}{-}C_{17} + C_{17}{-}C_{18})$	1198 vw	1245
$\nu(N_2{-}N_3)$	1175 m	1186
$\delta(C_{17}{-}$H ring E)	1167 m	1167
δ(C—H ring D)	1153 ms	1155
$\nu(C_8{-}O_3 + C_8{-}C_9) + \delta$(C—H rings A & D)	1133 w	1123
δ(C—H ring A)	1104 wm	1087
δ(C—H ring D)	1070 w	1066
$\nu(N_2{-}N_3) + \delta(C_7) + \delta$(rings A & D)	1059 m	1057
δ(ring A)	1044 ms	1033
δ(ring D)	1010 wm	1010
$\nu(V{=}O_1)$	958 vs	985
δ(ring E)	925 w	924
γ(C—H ring D)	902 w	902
γ(C—H ring D)	805 w	811
δ(rings A,B,C & D)	788 wm	778
γ(C—H ring D)	774 m	773
γ(C—H ring A)	746 w	751
γ(C—H ring A)	721 s	720
$\nu(V{-}O_4 + V{-}O_5)$	694 m	634
δ(ring A)	658 w	675
γ(ring E)	648 w	645
δ(ring E)	617 vw	608
$\nu(V{-}O_3)$	579 w	552
γ(ring E)	551 wm	538
δ(rings B & C)	499 vw	496
δ(rings A,B,C & D)	471 vw	458
$\nu(V{-}N_2)$	442 m	433
γ(ring A)	409 wm	420

Abbreviations for the band intensities: vw = very weak, w = weak, wm = weak-medium, m = medium, ms = medium-strong, s = strong, vs = very strong and sh = shoulder.
Attributions: ν = stretching, γ = out of plane deformation, δ = in plane deformation.

Table 5. Selected calculated bond lengths (pm) and angles (°) for [VO(acac)(apb)] *(1)*

Bond lengths		*Bond angles*	
V—O(1)	161.6	O(1)—V—N(1)	96.07
V—N(1)	212.7	O(1)—V—N(2)	101.72
V—N(2)	207.6	O(1)—V—O(3)	99.30
V—O(3)	204.0	O(1)—V—O(4)	100.56
V—O(4)	197.3	O(1)—V—O(5)	175.38
V—O(5)	227.4	N(1)—V—N(2)	76.15
C(6)—N(2)	131.8	N(1)—V—O(3)	149.59
N(2)—N(3)	134.6	N(1)—V—O(4)	99.05
N(3)—C(8)	134.5	N(1)—V—O(5)	79.62
C(8)—O(3)	129.8	N(2)—V—O(3)	75.13
C(8)—C(9)	148.4	N(2)—V—O(4)	157.58
C(16)—O(4)	129.8	N(2)—V—O(5)	75.13
C(18)—O(5)	127.1	O(3)—V—O(4)	103.68
C(16)—C(17)	140.0	O(3)—V—O(5)	83.85
C(17)—C(18)	142.1	O(4)—V—O(5)	81.87

structure, and for C(17) [6,2(3) pm] and N(21) [16,0(3) pm] in the two molecules of the triclinic modification. The complex geometry can be described as a distorted trigonal bipyramid formed by the VN_2O_3 moiety, with N(1) and O(3) in the axial and N(2), O(1) and O(2) in the equatorial positions. The appreciable deviation in the axial angle N(1)—V—O(3) (mean value of 146°) from the linearity is a consequence of steric constraints of the apb^{1-} ligand. Some differences between the angles involving the equatorial atoms in each structure modification are observed. While for the monoclinic structure the angles N(2)—V—O(1) and N(2)—V—O(2) are quite similar (mean value of 124°), for the two symmetry independent molecules in the triclinic modification the corresponding angles lie between 112 and 138°, showing a considerable variation. Hydrogen bonds of the O—H···C type (Figure 2) involving the oxo ligands are observed between the two crystallographic independent molecules.

Theoretically calculated structures and i.r. vibration bands of acetylacetonato(2-acetylpyridine-benzoylhydrazonato)-oxovanadium(IV) (1) and (2-acetylpyridine-benzoylhydrazonato)dioxovanadium(V) (2)

As a consequence of the oxidation process observed for complex *(1)* in solution, no X-ray suitable crystals of it could be obtained for a structure determination. Thus, it's molecular structure in a vacuum was calculated using molecular modeling and is shown in Figure 6. The complex's vibration bands were also calculated and compared with the observed i.r. data with good agreement (Table 4). Calculated bond lengths and angles for *(1)* are given in Table 5. The methodology was validated by comparison between bond angles and distances calculated and experimentally obtained data for complex *(2)*, whose crystal structure was determined. The theoretical and observed i.r. data (Table 6) are in good agreement, as well as the interatomic distances and angles, as shown in Table 2 and in Figure 1.

Supplementary material

Crystallographic data (excluding structure factors) have been deposited with the Cambridge Crystallographic Data Centre, under the deposition numbers CCDC 250081 for monoclinic and CCDC 250082 for the triclinic modification of $[VO_2(apb)]$ *(2)*. Copies of the data can be obtained free of charge on application to The Director, CCDC, 12 Union Road, Cambridge CB2, 1EZ, UK (Fax: +44-1223-336033; E-mail: deposit@ccdc.cam.ac.uk or www: http://www.ccdc.cam.ac.uk).

Table 6. Observed and calculated i.r. absorptions bands in the fingerprint region (1600–400 mm^{-1}) for [VO_2(apb)] *(2)*, whose structure with labeled rings is shown in Figure 1

Assignment	Obs.	Calcd.
$\nu(C_6{=}N_2 + C_{10}{=}C_{11} + C_{13}{=}C_{14})$	1598 ms	1594
$\nu(C_1{=}N_1 + C_1{=}C_2 + C_3{=}C_4 + C_4{=}C_5)$	1584 w	1590
ν(C=N + C=C rings A, B & D)	1568 w	1572
$\nu(C_6{=}N_2 + C_2{=}C_3)$	1507 ms	1545
$\nu(C_8{=}O_3 + C_8{=}N_3 + C_5{=}C_6)$ + δ(C—H ring A)	1495 m, sh	1484
$\nu(C_8{=}O_3 + C_8{-}C_9)$ + δ(C—H ring D)	1467 s	1473
$\nu(C_8{=}O_3)$ + δ(C—H rings A & D)	1436 vs	1442
$\nu(C_8{-}C_9 + C_6{-}C_7)$ + δ(C—H rings A & D)	1378 vs	1371
$\nu(C_1{-}N_1 + C_5{-}N_1 + C_8{-}N_3)$ + δ(C—H rings A & D)	1336 m	1325
$\nu(C_1{-}N_1 + C_5{-}N_1 + C_8{-}N_3)$ + δ(C—H rings A & D)	1307 m	1306
δ(C—H ring D)	1292 m	1282
δ(C—H ring A)	1266 wm	1273
$\nu(N_2{-}N_3)$	1179 m	1196
δ(C—H ring D)	1154 m	1160
$\nu(C_8{-}O_3)$ + δ(C—H rings A & D)	1138 w	1132
δ(C—H ring A)	1100 m	1097
δ(C—H rings A & D)	1065 m	1063
δ(ring A)	1048 w	1038
δ(ring D)	1033 m	1018
δ(ring A)	1012 w	1011
δ(ring B & C)	1000 w	992
	973 w	–
$\nu(V{=}O_1 + V{=}O_2)$	944 vs	985
γ(C—H ring D)	909 wm	917
$\delta(C_8$ ring C)	897 wm	890
γ(C—H ring A)	850 w	849
γ(C—H ring D)	793 wm	784
γ(rings A,B,C & D)	772 ms	779
γ(C—H ring A)	743 m	757
γ(C—H ring A)	705 s	725
$\nu(V{-}O_3)$ + δ(ring D)	692 ms	682
δ(ring A)	651 wm	650
δ(ring D)	596 m	610
$\nu(V{-}O_3)$	573 w	579
δ(rings B & C)	512 w	501
δ(rings A,B,C & D)	471 w	490
$\nu(V{-}N_2)$ + δ(rings B & C)	423 w	465
γ(ring A)	410 m	422

Abbreviations for the band intensities: vw = very weak, w = weak, wm = weak-medium, m = medium, ms = medium-strong, s = strong, vs = very strong and sh = shoulder.
Attributions: ν = stretching, γ = out of plane deformation, δ = in plane deformation.

Acknowledgements

The authors are grateful to Prof. Dr Dr h.c. J. Strähle (Tübingen) for the use of the X-ray diffractometers and acknowledge FINATEC, FAPESP and FINEP (CT INFRA 0970/01) for financial support and the CNPq for providing a scholarship to P.I.S.M.

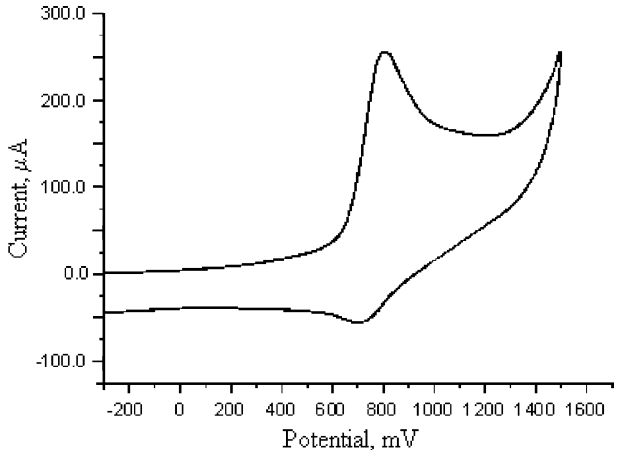

Fig. 4. Cyclic voltammogram of [VO(acac)(apb)] *(1) versus* Ag/AgCl in 0.1 M PTBA/CH_2Cl_2 and 100 mV s^{-1} scan rate.

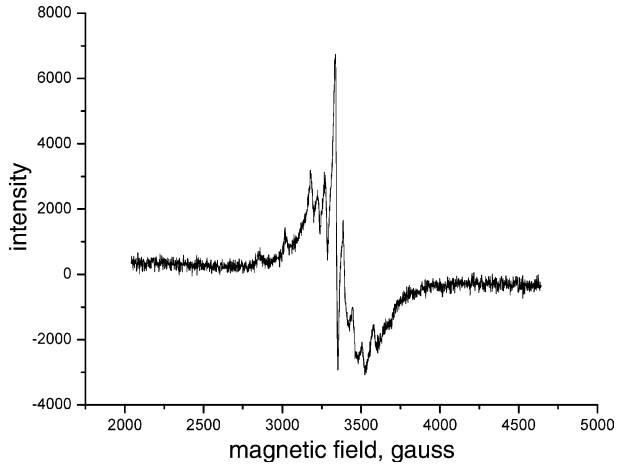

Fig. 5. Anisotropic e.p.r. spectrum of [VO(acac)(apb)] *(1)* in $CHCl_3$ at −196 °C.

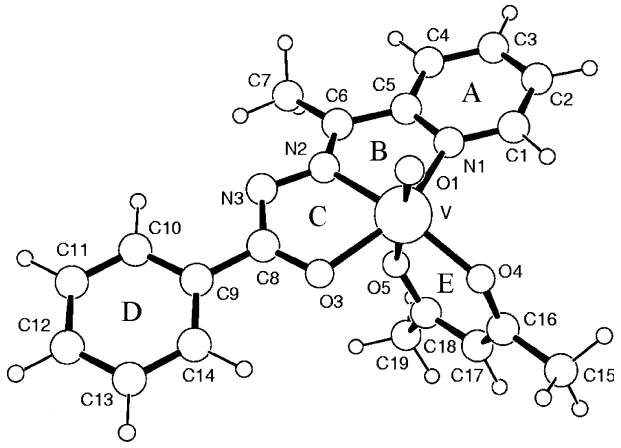

Fig. 6. Modeled molecular structure of [VO(acac)(apb)] *(1)* in a vacuum.

References

1. Y. Shechter, I. Goldwaser, M. Mironchik, M. Fridkin and D. Gefel, *Coord. Chem. Rev.*, **237**, 3 (2003).
2. D. Rehder, *Inorg. Chem. Comm.*, **6**, 604 (2003).
3. K.H. Thompson and C. Orvig, *Coord. Chem. Rev.*, **219**, 1033 (2001).
4. G. Verquin, G. Fontaine, M. Bria, E. Zhilinskaya, E. Abi-Aad, A. Aboukais, B. Baldeyrou, C. Bailly and J.L. Bernier, *J. Biol. Inorg. Chem.*, **9**, 345 (2004).

5. N. Raman, A. Kulandaisamy and K. Jeyasubramanian, *Synt. Reac. Inorg. Met-Org. Chem.*, **34**, 17 (2004).
6. V.M. Deflon, D.M. de Oliveira, G.F. de Sousa, A.A. Batista, L.R. Dinelli and E. Castellano, *Z. Anorg. Allg. Chem.*, **628**, 1140 (2002).
7. J. Patole, U. Sandbhor, S. Padhye, D.N. Deobagkar, C.E. Anson and A. Powell, *Bioorg. Med. Chem. Lett.*, **13**, 51 (2003).
8. M.R. Maurya, S. Khurana, W. Zhang and D. Rehder, *J. Chem. Soc. Dalton Trans.*, 3015 (2002).
9. W. Kraus and G. Nolze, *J. Appl. Cryst.*, **29**, 301 (1996).
10. A. Boultif and D. Louer, *J. Appl. Cryst.*, **24**, 987 (1991).
11. A.L. Spek, PLATON, A Multipurpose Crystallographic Toll, University of Utrecht, The Netherlands, 2003.
12. A. Altomare, G. Cascarano, C. Giacovazzo, A. Gualardi, *J. Appl. Cryst.*, **26**, 343 (1993).
13. G.M. Sheldrick, SHELXS97, Program for the solution of crystal structures, University of Göttingen, Germany, 1997.
14. G.M. Sheldrick, SHELXL97, Program for the refinement of crystal structures, University of Göttingen, Germany, 1997.
15. W.J. Hehre, J. Yu, P.E. Klunzinger and L. Lou, A Brief Guide to Molecular Mechanics and Quantum Chemical Calculations, Wavefunction Inc., Irvine CA, 1998, p. 17 and 21.
16. P.C. Spartan Pro v1.0.5, Wavefunction Inc., 18401 Von Karman Ave., Suite 370, Irvine, CA 92612 (www.wavefun.com).

TMCH 6114